bioRxiv preprint doi: https://doi.org/10.1101/622662; this version posted April 29, 2019. The copyright holder for this preprint (which was not certified by peer review) is the author/funder, who has granted bioRxiv a license to display the preprint in perpetuity. It is made available under aCC-BY 4.0 International license.

Morphogenesis and dynamics of slime molds in various environments

Fernando Patino-Ramirez [1*] , Aurèle Boussard[2], Chloé Arson[1¶], Audrey Dussutour[2¶*]

[1] School of Civil and Environmental Engineering, Georgia Institute of Technology, Atlanta, GA, USA

[2] Research Centre on Animal Cognition (CRCA), Centre for Integrative Biology (CBI), Toulouse University, CNRS, UPS, Toulouse, France

* Corresponding authors

E-mails: fp@gatech.edu (FP), audrey.dussutour@univ-tlse3.fr (AD)

¶ These authors contributed equally to this work.

bioRxiv preprint doi: https://doi.org/10.1101/622662; this version posted April 29, 2019. The copyright holder for this preprint (which was not certified by peer review) is the author/funder, who has granted bioRxiv a license to display the preprint in perpetuity. It is made available under aCC-BY 4.0 International license.

Abstract

Cells, including unicellulars, are highly sensitive to external constraints from their environment. Amoeboid cells change their cell shape during locomotion and in response to external stimuli. Physarum polycephalum is a large multinucleated amoeboid cell that extends and develops pseudopods. In this paper, changes in cell behavior and shape were measured during the exploration of homogenous and non-homogenous environments that presented neutral, and nutritive and/or adverse substances. In the first place, we developed a fully automated image analysis method to measure quantitatively changes in both migration and shape. Then we measured various metrics that describe the area covered, the exploration dynamics, the migration rate and the slime mold shape. Our results show that: 1) Not only the nature, but also the spatial distribution of chemical substances affect the exploration behavior of slime molds; 2) Nutritive and adverse substances both slow down the exploration and prevent the formation of pseudopods; and 3) Slime mold placed in an adverse environment preferentially occupies previously explored areas rather than unexplored areas using mucus secretion as a buffer. Our results also show that slime molds migrate at a rate governed by the substrate up until they get within a critical distance to chemical substances.

Key words: Morphogenesis, Slime molds, Nutritive/adverse environments, Image analysis, Migration rate, Growth, Exploration

bioRxiv preprint doi: https://doi.org/10.1101/622662; this version posted April 29, 2019. The copyright holder for this preprint (which was not certified by peer review) is the author/funder, who has granted bioRxiv a license to display the preprint in perpetuity. It is made available under aCC-BY 4.0 International license.

Author summary

Physarum polycephalum, also called slime mold, is a giant single-celled organism that can grow to cover several square meters, forming search fronts that are connected to a system of intersecting veins. An original experimental protocol allowed tracking the shape of slime mold placed in homogenous substrates containing an attractant (glucose) or a repellent (salt), or inhomogeneous substrates that contained an attractive spot (glucose), an eccentric slime mold and a repulsive spot (salt) in between. For the first time, the rate of exploration of unexplored areas (primary growth) and the rate of extension in previously explored areas (secondary growth) were rigorously measured, by means of a sophisticated image analysis program. This paper shows that the chemical composition of the substrate has more influence on the morphology and growth dynamics of slime mold than that of concentrated spots of chemicals. It was also found that on a repulsive substrate, slime mold exhibits a bias towards secondary growth, which suggests that the mucus produced during slime mold migration acts as a protective shell in adverse environments.

Introduction

Large-scale spatial patterns in biology are common and knowing how these patterns evolve and what are their functional role, enables us to understand the evolution of biocomplexity (see e.g. (1–4)). Morphogenesis has been studied in length at the cell level (see e.g (5–8)); cells are highly sensitive to geometrical and mechanical constraints from their microenvironment and respond to these conditions by

bioRxiv preprint doi: https://doi.org/10.1101/622662; this version posted April 29, 2019. The copyright holder for this preprint (which was not certified by peer review) is the author/funder, who has granted bioRxiv a license to display the preprint in perpetuity. It is made available under aCC-BY 4.0 International license.

changing shape (see e.g. (9,10)); these transformations impact cell migration and growth (see e.g. (7,11–13)). Cellular migration is a fundamental property of every cell and it is crucial for the development and morphogenesis of animal body plans and organ systems (see e.g. (14–16)). Cell migration is either in a random direction or directed towards localized cues (17–20). Mechanisms of cellular movement have been mostly studied in chemotactic cells, such as neutrophils (17), bacteria (21), Ciliata (22), fungi (23) and cellular slime molds (19).

Due to its extremely fast migration rate and highly irregular shape, the acellular slime mold *Physarum Polycephalum* represents a prime example of differentiated growth and thus offers an attractive model for the analysis of morphogenesis dynamics underlying cellular migration and exploration (24–28). *P polycephalum* is a giant single-celled organism that can grow to cover several square meters. Its morphology includes search fronts that are connected to a system of intersecting veins, in which oscillatory flows of the protoplasm “shuttle streaming” take place. This vein network allows 1) an efficient distribution of chemical signals, oxygen, nutrients over large distances and 2) cell migration at a speed of few centimeters per hour (29,30). The driving force for this protoplasm streaming is a periodic, peristaltic contraction and relaxation of the veins due to the actin-myosin interaction, which is regulated by oscillations of intracellular chemicals such as calcium (31–33). As it explores its environment, the slime mold extends temporary arm-like projections named pseudopods. It also secretes continuously a thick extracellular slime (34). The glycoprotein nature of the extracellular slime coat endows *P polycephalum* with unique protective and structural properties that favor survival of the migrating, naked

bioRxiv preprint doi: https://doi.org/10.1101/622662; this version posted April 29, 2019. The copyright holder for this preprint (which was not certified by peer review) is the author/funder, who has granted bioRxiv a license to display the preprint in perpetuity. It is made available under aCC-BY 4.0 International license.

slime mold (35). As the slime mold is foraging, it avoids areas covered with this mucus, which marks previously explored areas (36,37).

In the presence of chemical substances in the environment, *P. Polycephalum* shows directional movements towards or away from the stimuli (i.e. chemotaxis). *Physarum* morphology, evolution and behaviors are strongly affected by the availability, location and concentration of nutrients. When the slime mold senses attractants (e.g. food cues) using specific receptors located on the membrane, the oscillation frequency in the pseudopod closest to the attractant increases, causing cytoplasm to flow towards the attractant (38). On the contrary, when repellents such as salts are sensed, the oscillation frequency decreases and the slime mold moves away from the repellent (38). Although slime molds lack the complex hardware of animals with brains, they live in environments that are as complex and they face the same decision-making challenges (39). Hence, acellular slime molds have been the subject of a wide range of studies showing that they can solve complex biological and computational problems without any specialized nervous tissue (24,36,37,40–45).

In this paper the objectives are to characterize the morphology and dynamics of *Physarum* exploring various environments. First, we investigate how movement is affected by homogeneous environmental conditions: adverse environment (using salt as a repellent (46); nutritive environments (using glucose as a chemo-attractant (47,48) with 2 different concentrations) and a neutral environment (using plain agar). Second, we analyze the geometrical evolution of slime molds placed at a distance from a nutritive spot (glucose), with and without a repelling spot (salt) in between. We characterize slime molds' movement both temporally and spatially, to capture the

bioRxiv preprint doi: https://doi.org/10.1101/622662; this version posted April 29, 2019. The copyright holder for this preprint (which was not certified by peer review) is the author/funder, who has granted bioRxiv a license to display the preprint in perpetuity. It is made available under aCC-BY 4.0 International license.

full dynamics. To this aim, we develop a program that automatically analyzes sequences of images to track the areas covered and explored by the slime mold, the slime mold shape, the refinement and secondary growth cycles, as well as the distance to the nutritive spot.

Results

1) Homogeneous environment

In order to study the influence of the environment on slime mold expansion rate, we analyzed the areas covered by slime mold, unexplored substrate and mucus over time, as shown in Fig 1.

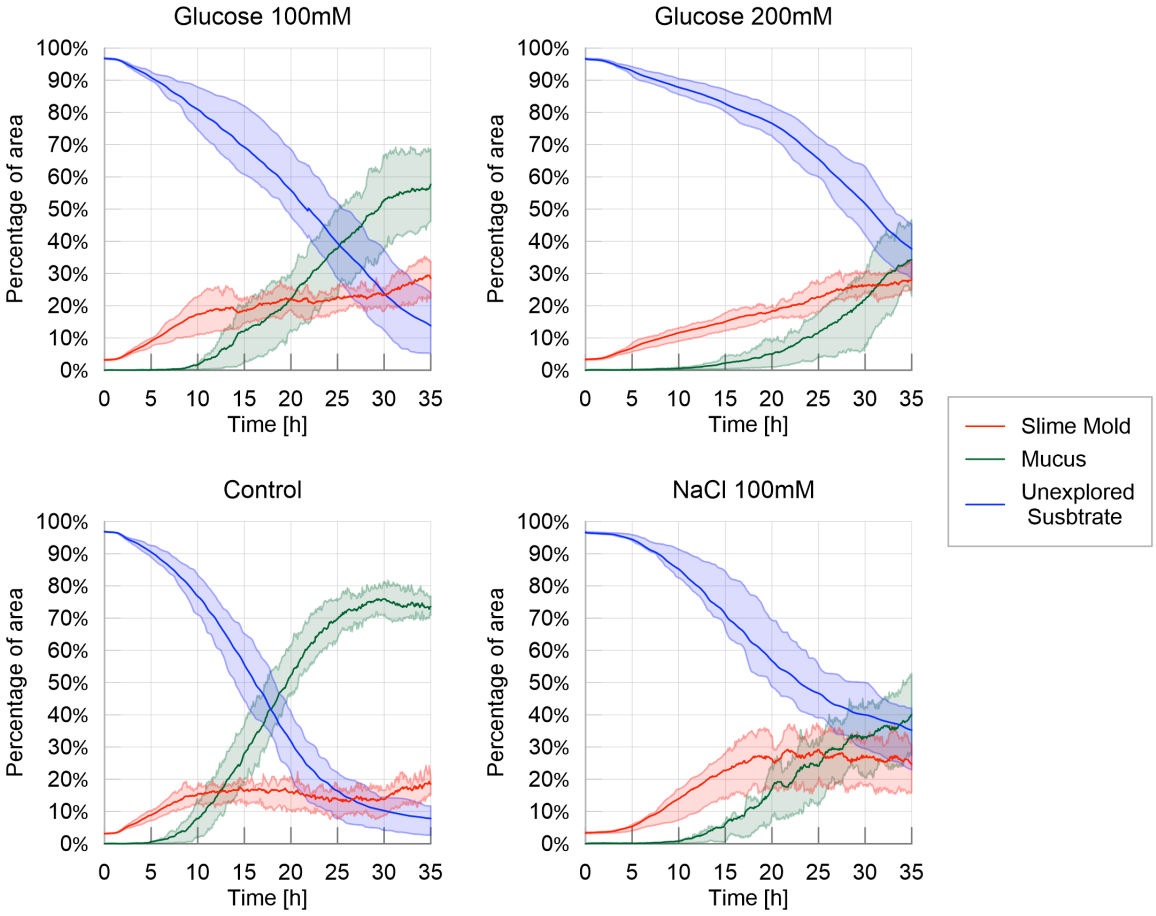

bioRxiv preprint doi: https://doi.org/10.1101/622662; this version posted April 29, 2019. The copyright holder for this preprint (which was not certified by peer review) is the author/funder, who has granted bioRxiv a license to display the preprint in perpetuity. It is made available under aCC-BY 4.0 International license.

Fig 1. Fraction of area covered by slime mold, mucus and unexplored substrate – Homogeneous environment. The solid line corresponds to the average index calculated over the 20 replicates, while the shaded areas correspond to the first and third quartiles of the data.

In a neutral (control) and slightly nutritive environment (glucose at 100 mM), the slime molds started to spread from the very beginning of the experiment (Fig 1; Table 1 and Fig 5 in S1 Appendix, $P>0.05$). In contrast in a highly nutritive environment (200 mM glucose), slime molds started to explore later ($P<0.001$ when compared to the control). Slime molds placed in an adverse environment (100 mM NaCl) were lagging the most and only started exploring after 3 hours ($P<0.001$ when compared to the control). Once the slime molds started to explore, they all grew at the same rate (Fig 1; Table 2, Fig 6 in S1 Appendix, $P> 0.05$ when compared to the control) except the ones placed in a highly nutritive environment which were slowed down ($P<0.001$ when compared to the control).

At the end of the experiment (after 35 hours), the slime molds reached a similar surface in a control environment and in an adverse environment (Table 3 and Fig 7 in S1 Appendix , $P>0.05$ when compared to the control). Interestingly, after reaching a plateau at 18 hours, the area covered by the slime molds in an adverse environment oscillated with seemingly cyclic fluctuations (Fig 1). In both a slightly and a highly nutritive environment, the slime molds reached a higher final surface than the slime molds placed in a control environment ($P<0.001$ in both comparisons) and covered approximately 30% of arena at the end experiment. It is worth noting that in a highly nutritive environment, the surface covered by the slime molds never reached a plateau after 35 hours, suggesting that the slime molds did not reach its maximum surface (Fig 1).

bioRxiv preprint doi: https://doi.org/10.1101/622662; this version posted April 29, 2019. The copyright holder for this preprint (which was not certified by peer review) is the author/funder, who has granted bioRxiv a license to display the preprint in perpetuity. It is made available under aCC-BY 4.0 International license.

Refinement *i.e.* appearance of mucus, was observed after 5 hours in the control environment. In all other environments, mucus appeared later (Table 4 and Fig 8 in S1 Appendix: $P<0.001$ for all treatments when compared to the control). In a highly nutritive environment, mucus was only observed after 10 hours, which marked the strongest delay in the refinement process. Once the mucus started to be apparent, its surface grew quicker in the control environment than in the other three treatments (Table 5 and Fig 9 in S1 Appendix; $P<0.001$ for all treatments when compared to the control). Thus the surface covered by mucus at the end of the experiment was the largest in the control environment where it reached 75% of the arena against 55%, 40% and 35% for the slightly nutritive, the adverse and the highly nutritive environments respectively (Table 6 and Fig 10 in S1 Appendix; $P<0.001$ for all treatments when compared to the control).

Hence, slime molds placed in a control environment explored almost all the arena leaving only 5% of the arena unexplored while in the other treatments the surface unexplored were significant: 15%, 35% and 38% for the slightly nutritive, the highly nutritive and the adverse environments respectively. Interestingly, although the growth rate dynamics differed between highly nutritive and adverse environments, the final unexplored surfaces were similar. In a highly nutritive environment the slime molds grew slowly and steadily while in an adverse environment slime molds grew rather quickly but after a long delay.

Next, we analyzed the evolution of the cumulative areas covered by primary growth, refinement and secondary growth (Fig 2). The cumulative area covered by secondary growth, which reveals the cyclic nature of the exploration process, was

bioRxiv preprint doi: https://doi.org/10.1101/622662; this version posted April 29, 2019. The copyright holder for this preprint (which was not certified by peer review) is the author/funder, who has granted bioRxiv a license to display the preprint in perpetuity. It is made available under aCC-BY 4.0 International license.

the highest in the adverse environment (480% coverage) followed by the control environment (380%), the slightly nutritive environment (250%) and the highly nutritive environment (180%). All comparisons lead to significant differences $P<0.05$, except control vs. adverse environment (Table 7 and Fig 11 in S1 Appendix). This observation confirms that exploration was slowed down by the presence of nutrients, and that the pulsatile behavior (*i.e* the exploration of previously explored area) was stimulated by repellents.

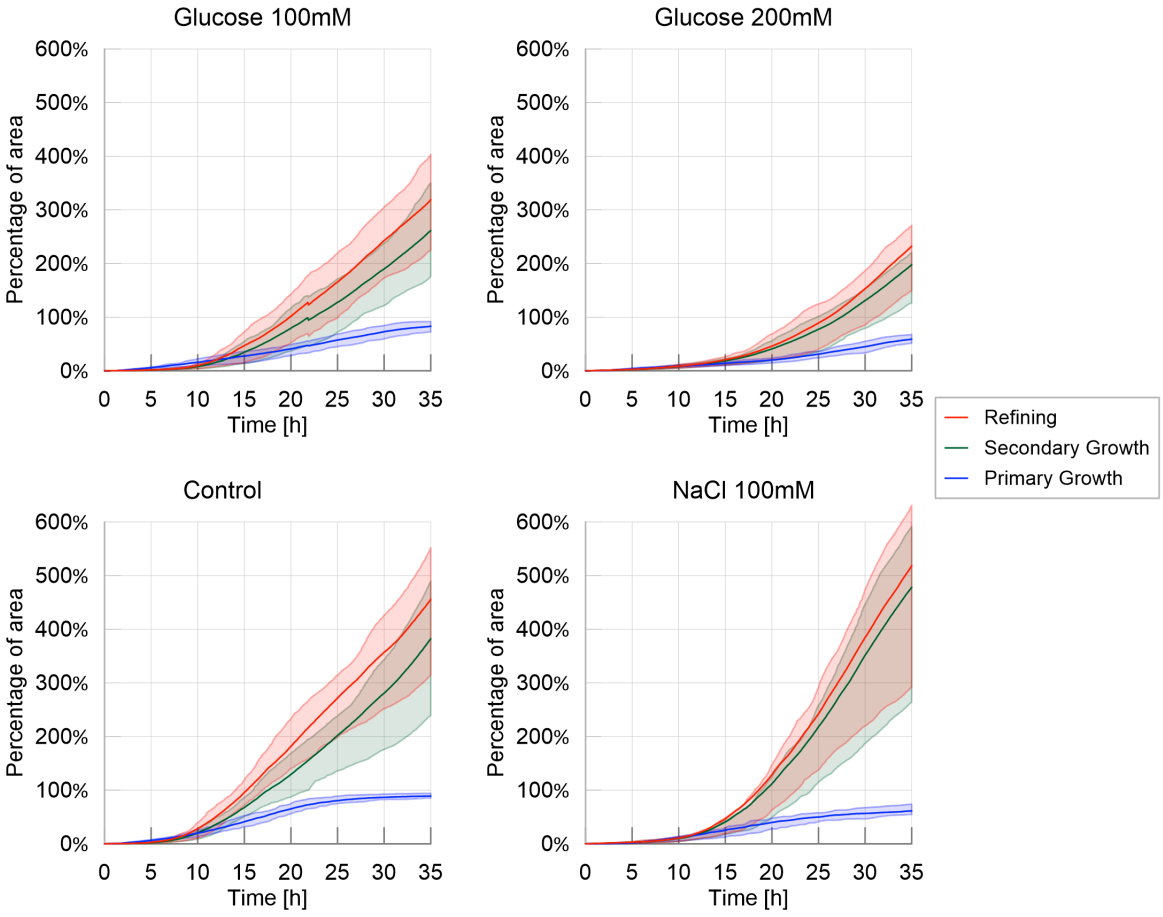

Fig 2. Cumulative areas covered by primary growth, refinement and secondary growth – Homogeneous experiments. The solid line corresponds to the average index calculated over the 20 replicates, while the shaded areas correspond to the first and third quartiles of the data.

bioRxiv preprint doi: https://doi.org/10.1101/622662; this version posted April 29, 2019. The copyright holder for this preprint (which was not certified by peer review) is the author/funder, who has granted bioRxiv a license to display the preprint in perpetuity. It is made available under aCC-BY 4.0 International license.

202 In accordance with the previous results, the migration rate was higher for the control
203 treatment than for the other treatments (Table 8 and Fig 12 in S1 Appendix: P<0.001
204 for each pairwise comparison). While slime molds exploring the highly nutritive
205 environment were slower than slime molds exploring the slightly nutritive or the
206 adverse environment (P<0.001 each), these two showed no significant differences
207 (P>0.05).

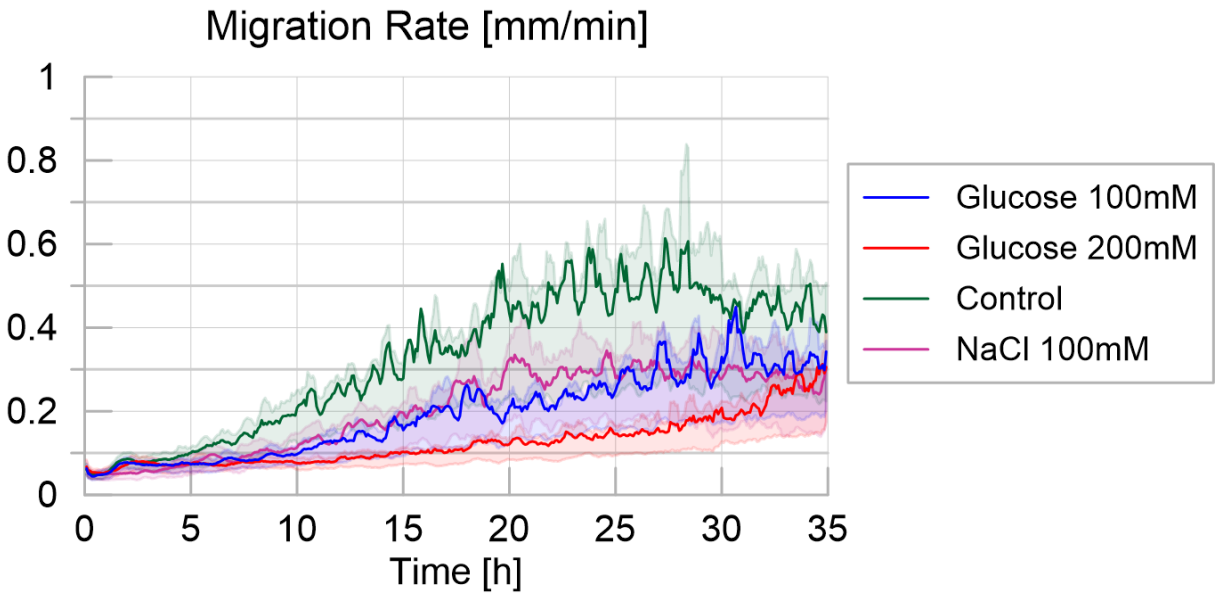

208
209

210 Fig 3: Migration rate over time for the four different treatments, defined as the maximum distance
211 between the contours of the slime mold between two consecutive images divided by their time interval
212 (5 minutes apart), measured in millimeters per minute. The solid line corresponds to the average
213 calculated over 20 replicates per treatment, while the shaded areas correspond to the first and third
214 quartiles of the data.

215

216 The slime molds exploring the adverse environment showed the highest probability
217 to explore a previously explored substrate than the other treatments as shown in Fig
218 4 and supplementary materials (Tendency for secondary growth: Table 9 and Fig 13
219 in S1 Appendix: P<0.001 for each pairwise comparison). When exploring a highly
220 nutritive environment, slime molds also displayed a significant positive tendency for

bioRxiv preprint doi: https://doi.org/10.1101/622662; this version posted April 29, 2019. The copyright holder for this preprint (which was not certified by peer review) is the author/funder, who has granted bioRxiv a license to display the preprint in perpetuity. It is made available under aCC-BY 4.0 International license.

221 secondary growth (P<0.001 for each pairwise comparison) but significantly less
222 strong than on the adverse environment (P<0.001). For the others treatments, the
223 measured proportion of secondary growth was not different from the expected
224 proportion of secondary growth, indicating that the slime molds did not avoid
225 previously explored substrate and explored randomly (Fig 13 in S1 Appendix). The
226 peaks observed within the first 5 hours of the experiment correspond to an isotropic
227 extension immediately followed by a refinement process that occurred before the
228 slime mold started to explore continuously its environment. This behavior is often
229 observed when a slime mold is introduced in a new environment and is referred as
230 “contemplative” (49) *i.e.* the slime mold migrates, retracts and moves again. The
231 peak was larger for adverse environment.
232

bioRxiv preprint doi: https://doi.org/10.1101/622662; this version posted April 29, 2019. The copyright holder for this preprint (which was not certified by peer review) is the author/funder, who has granted bioRxiv a license to display the preprint in perpetuity. It is made available under aCC-BY 4.0 International license.

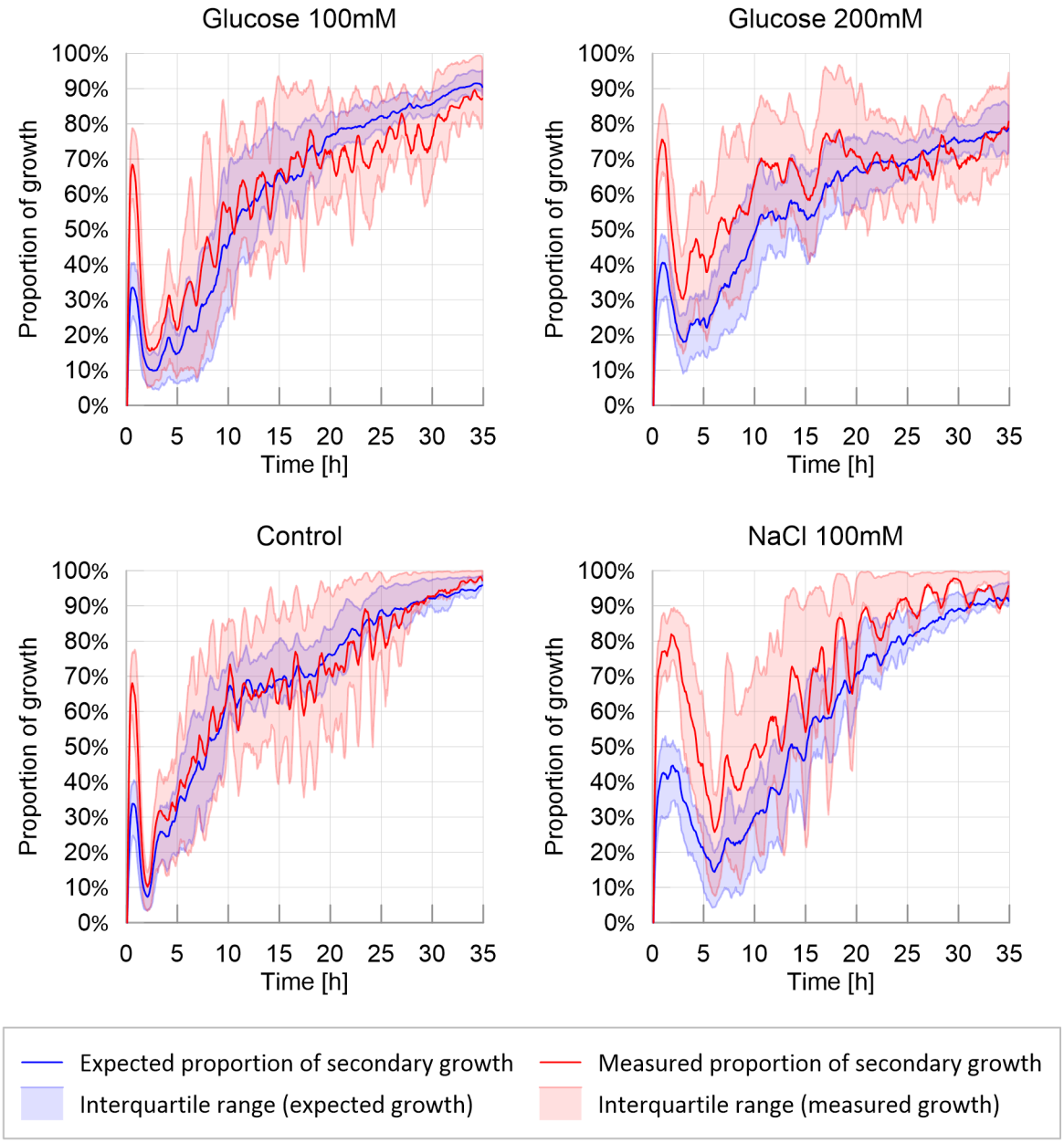

Fig 4: Ratio of secondary growth: observed and expected proportion of secondary growth. The solid line corresponds to the average calculated over 20 replicates per treatment, while the shaded areas correspond to the first and third quartiles of the data.

We then analyzed the evolution of the shape of the slime molds contour. Note that the experimental set ups in which slime molds were placed exhibited radial symmetry. Hence, no preferential expansion direction was expected. We thus focused on contour shape, not orientation.

bioRxiv preprint doi: https://doi.org/10.1101/622662; this version posted April 29, 2019. The copyright holder for this preprint (which was not certified by peer review) is the author/funder, who has granted bioRxiv a license to display the preprint in perpetuity. It is made available under aCC-BY 4.0 International license.

As expected, circularity was initially one in all tests (circular slime mold spot), and increased over time as the contour shape departed from a circle (Fig 2 in S1 Appendix). In the control and nutritive environments, circularity remained between 1.05 and 1.10, whereas it fluctuated between 1.05 and 1.30 in the adverse environment. This observation suggests that, in an adverse environment, slime molds explored the petri dish by spreading and thinning over larger areas than in the other environments, which led to shape changes and a decrease of slime mold circularity. However fluctuations among the 20 replicates were too high to identify any trend in the evolution of slime mold circularity.

The eccentricity index was initially close to zero (circular cell) and increased up to almost 0.8 over time, with important fluctuations in all the treatments (Fig 3 in S1 Appendix). Eccentricity is an indicator of the number of pseudopodia. But a non-eccentric convex hull can enclose non-circular contours of slime mold, since pseudopodia can develop in a symmetric fashion. That is why no major difference was noted between the treatments. This result highlights the absence of preferred expansion direction in symmetric, homogeneous environments.

Solidity decreased with the emergence of pseudopodia, since slime mold branching disrupted the initially convex shape of the slime mold (Fig 5). In the control environment, in which the exploration rate was the highest, the decrease of solidity of the slime mold area was the highest (and the fastest) decreasing from 1 to 0.3 and then becoming relatively stable, with fluctuations of +/- 0.05 (Table 10 and Fig 14 in S1 Appendix; $P<0.01$ for all paired comparisons except adverse environment vs. slightly nutritive environment, where $P>0.05$). Slower exploration resulted in a slower and steadier loss of solidity as observed in the nutritive and adverse environments.

bioRxiv preprint doi: https://doi.org/10.1101/622662; this version posted April 29, 2019. The copyright holder for this preprint (which was not certified by peer review) is the author/funder, who has granted bioRxiv a license to display the preprint in perpetuity. It is made available under aCC-BY 4.0 International license.

The highly nutritive environment yielded the highest solidity at the end of the experiment (0.6), which confirmed that the presence of glucose slowed down exploration.

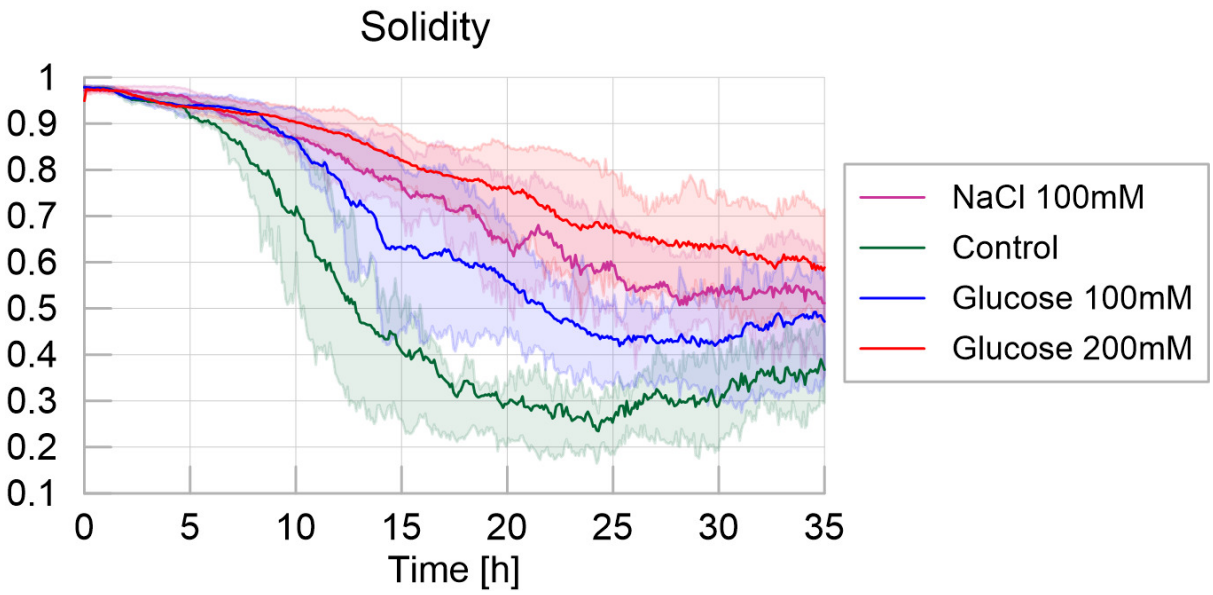

Fig 5. Solidity - Homogeneous experiments. The solid line corresponds to the average index calculated over the 20 replicates, while the shaded areas correspond to the first and third quartiles of the data.

We next focused on the number of clusters, corresponding to the number of pseudopodia (Fig 6). Initially the slime molds stretched as a single cluster. Once mucus started to be apparent, slime molds usually divided up into several clusters, and started the active exploration phase. In highly nutritive and adverse environments, the number of clusters over time was lower than in the other two treatments (new pseudopod number: Table 11 and Fig 15 in S1 Appendix, and $P < 0.01$ for all paired comparisons except for adverse environment vs. highly nutritive environment). This observation confirmed that the presence of concentrated nutrients slowed down the exploration, and that the presence of repellents triggered

bioRxiv preprint doi: https://doi.org/10.1101/622662; this version posted April 29, 2019. The copyright holder for this preprint (which was not certified by peer review) is the author/funder, who has granted bioRxiv a license to display the preprint in perpetuity. It is made available under aCC-BY 4.0 International license.

285 a highly pulsatile behavior with small exploration fronts, which were sometimes not
286 detected as separate clusters.
287

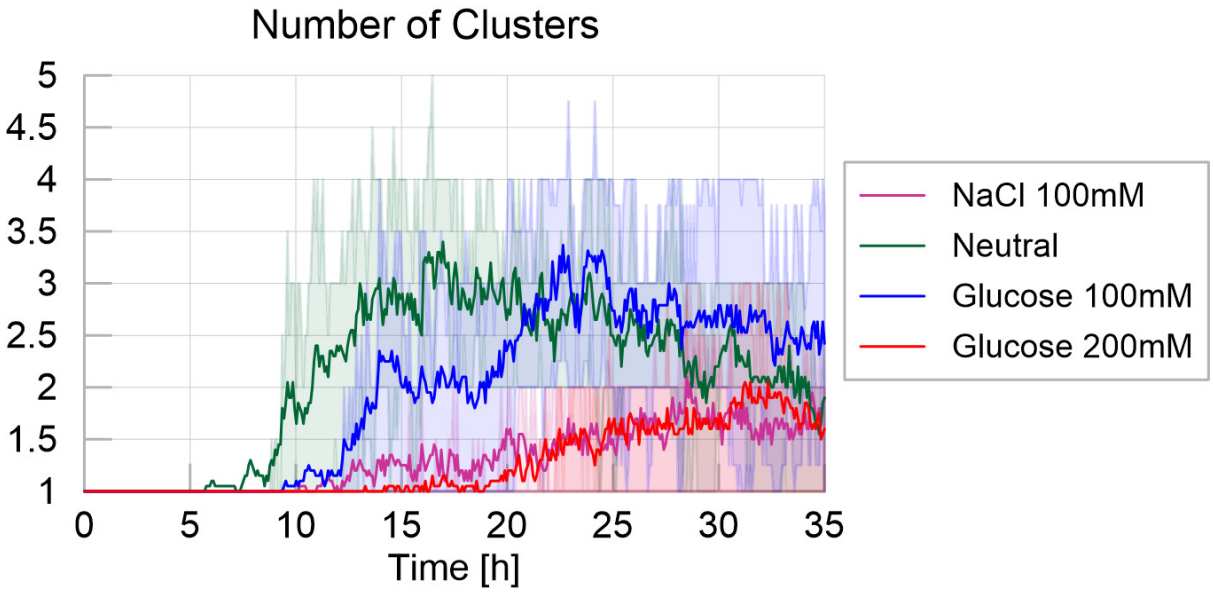

288

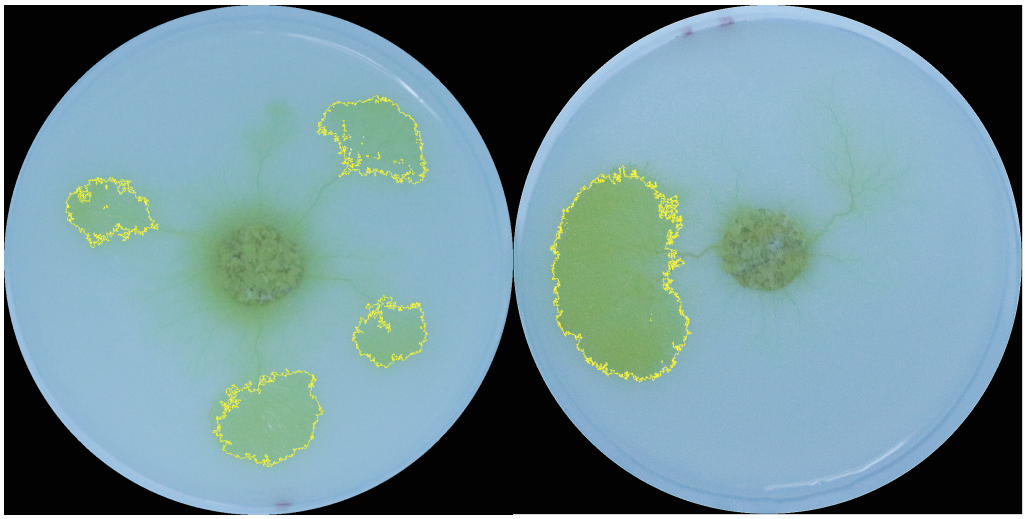

289

290 Fig 6. Number of clusters - Homogeneous experiments. The solid line corresponds to the average
291 index calculated over the 20 replicates, while the shaded areas correspond to the first and third
292 quartiles of the data. Pictures show examples of clusters for the Control environment (left) and
293 200mM Glucose environment (right).
294
295
296

bioRxiv preprint doi: https://doi.org/10.1101/622662; this version posted April 29, 2019. The copyright holder for this preprint (which was not certified by peer review) is the author/funder, who has granted bioRxiv a license to display the preprint in perpetuity. It is made available under aCC-BY 4.0 International license.

297 **2) Spot experiments**

298 In the spot experiments, we studied the influence of discrete distributions of nutrients
299 and repellents on exploration dynamics. When looking at the evolution of slime mold,
300 mucus and unexplored substrate over time (Fig 7), we only observed marginal
301 difference among the treatments, which all exhibited similar patterns of exploration,
302 e.g. similar percentage of non-explored area and similar mucus accumulation. The
303 presence of an adverse spot only delayed the appearance of the first pseudopod
304 (first movement: Table 12 and Fig 15 in S1 Appendix, $P<0.05$) but not the first
305 appearance of mucus (first appearance of mucus: Table 15 in S1 Appendix, not
306 significant). The only noticeable differences lie in the surface reached at the end of
307 the experiment: slime molds that were offered a highly nutritive spot grew larger
308 (final surface: Table 14 and Fig 17 in S1 Appendix; $P < 0.01$). By contrast, the
309 surface covered by mucus was lower (mucus final surface: Table 17 and Fig 18 in
310 S1 Appendix; $P <0.01$) than slime molds that were offered a slightly nutritive spot. In
311 comparison with the experiments conducted in homogeneous environments, we did
312 not observe any expansion/refinement cycles in the spot experiments, meaning that
313 slime mold spread steadily towards the food source despite the presence of an
314 obstacle on the way.
315

bioRxiv preprint doi: https://doi.org/10.1101/622662; this version posted April 29, 2019. The copyright holder for this preprint (which was not certified by peer review) is the author/funder, who has granted bioRxiv a license to display the preprint in perpetuity. It is made available under aCC-BY 4.0 International license.

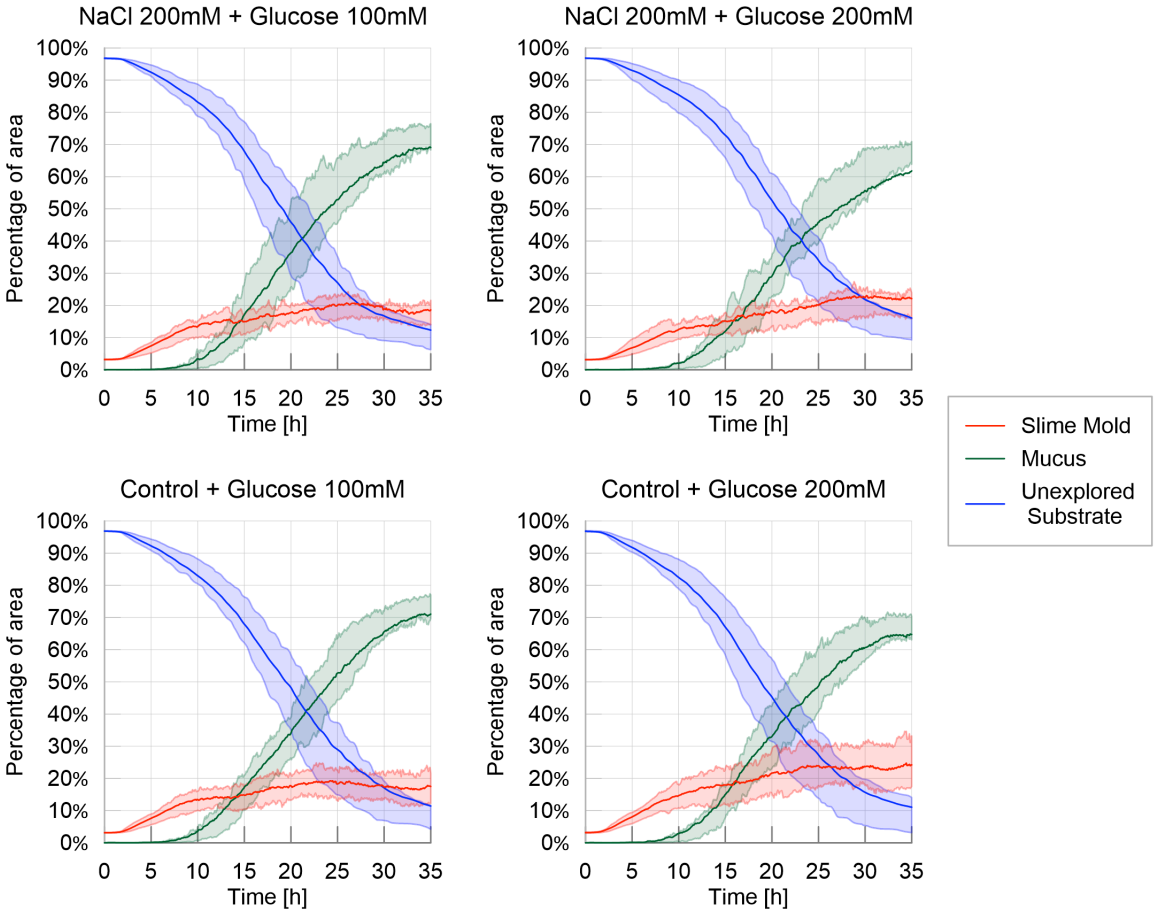

Fig 7. Fraction of area covered by each entity (slime mold, mucus, unexplored substrate) – Spot experiments. The solid line corresponds to the average index calculated over the 20 replicates, while the shaded areas correspond to the first and third quartiles of the data

The exploration behavior in the spot experiments was similar to that observed in the control environment in homogeneous experiments as observed in Fig 8, which includes the average percentage of unexplored area for the homogeneous and spot experiments shown in Fig 1 and Fig 7 respectively. This suggests that the spatial exploration of slime mold depended mostly on the substrate and not on the geometric distribution of the nutritive and adverse stimuli.

bioRxiv preprint doi: https://doi.org/10.1101/622662; this version posted April 29, 2019. The copyright holder for this preprint (which was not certified by peer review) is the author/funder, who has granted bioRxiv a license to display the preprint in perpetuity. It is made available under aCC-BY 4.0 International license.

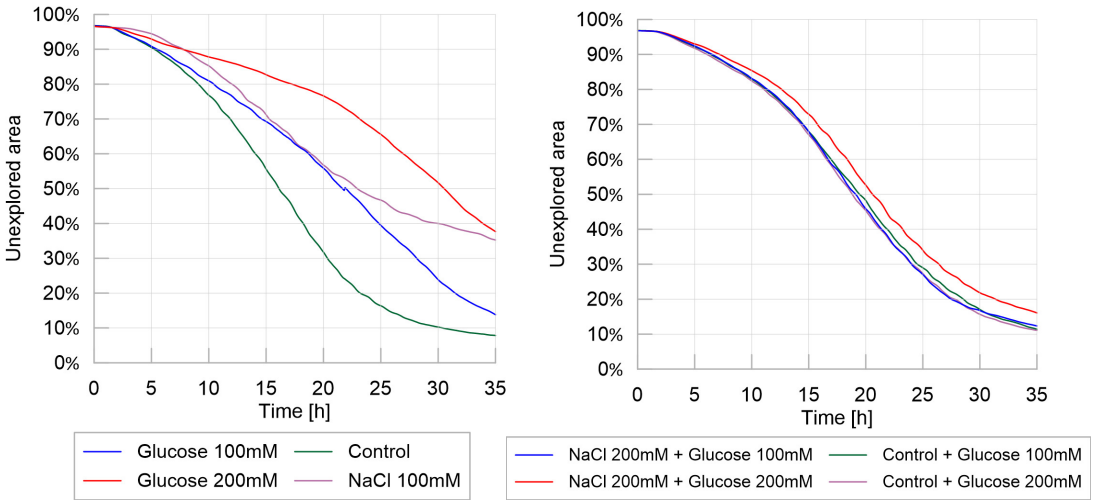

Fig 8. Exploration behavior: homogeneous experiments (left) vs. spot experiments (right). Percentage of unexplored area over time. Mean values of over 20 replicates for each different treatment.

The cumulative areas covered by secondary growth for the spot experiments (Fig 9) were also similar for all treatments (Table 18 in S1 Appendix, P >0.05), suggesting again, that isolated spots with nutritive or adverse stimuli did not alter the overall exploration of slime molds when growing on the same, control, substrate.

bioRxiv preprint doi: https://doi.org/10.1101/622662; this version posted April 29, 2019. The copyright holder for this preprint (which was not certified by peer review) is the author/funder, who has granted bioRxiv a license to display the preprint in perpetuity. It is made available under aCC-BY 4.0 International license.

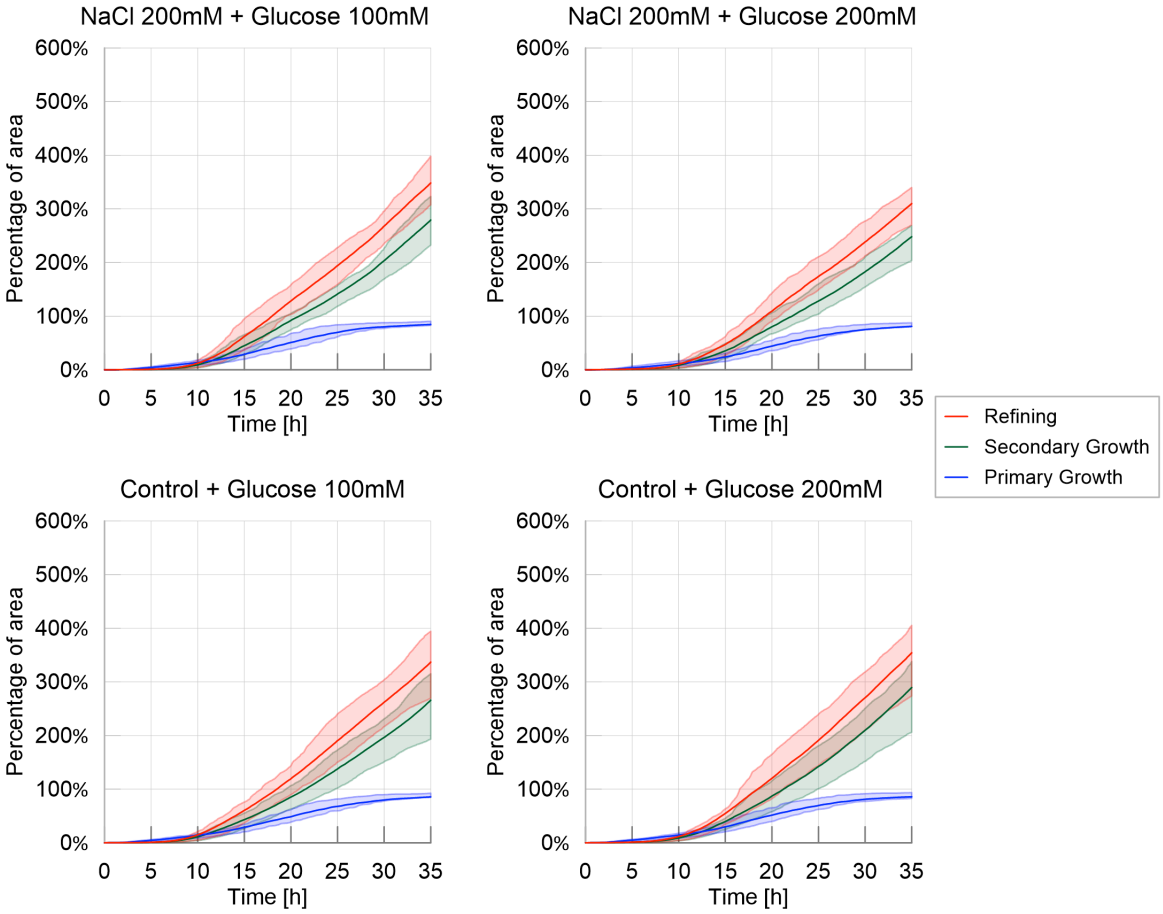

337

338 Fig 9. Cumulative areas covered by primary growth, refinement and secondary growth – Spot
339 experiments. The solid line corresponds to the average index calculated over the 20 replicates, while
340 the shaded areas correspond to the first and third quartiles of the data

341

342 The trends of migration rate, as shown in Fig 10, show that slime molds were not
343 affected by the difference between treatments, showing only a slight effect of the
344 concentration of the food spot ($P<0.05$), as shown on Table 19 in S1 Appendix. This
345 effect showed that the migration rate was slightly superior when slime molds were
346 offered a higher than a lower nutritive spot.

bioRxiv preprint doi: https://doi.org/10.1101/622662; this version posted April 29, 2019. The copyright holder for this preprint (which was not certified by peer review) is the author/funder, who has granted bioRxiv a license to display the preprint in perpetuity. It is made available under aCC-BY 4.0 International license.

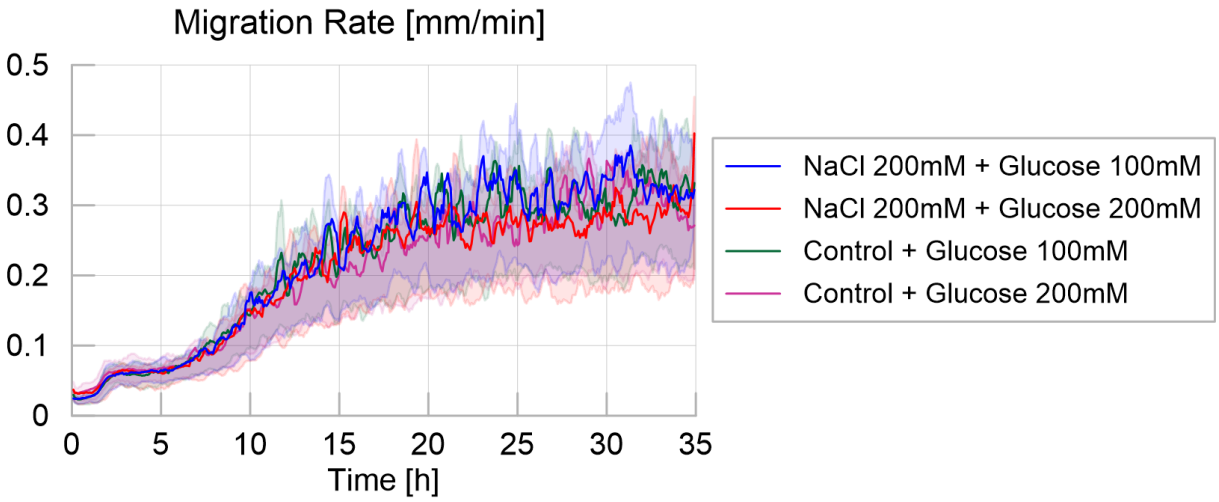

Fig 10: Migration rate over time for the four different treatments, defined as the maximum distance between the contours of the slime mold between two consecutive images, divided by their time interval (5 minutes apart), measured in millimeters per minute. The solid line corresponds to the average calculated over 20 replicates per treatment, while the shaded areas correspond to the first and third quartiles of the data.

Similarly, looking at the predilection of slime molds to grow towards mucus (secondary growth), as shown in Fig 11, no significant differences were observed between treatments (Table 19 in S1 Appendix), which suggests that the growth type is not influenced by the existence or concentration of discrete attracting/repelling spots.

bioRxiv preprint doi: https://doi.org/10.1101/622662; this version posted April 29, 2019. The copyright holder for this preprint (which was not certified by peer review) is the author/funder, who has granted bioRxiv a license to display the preprint in perpetuity. It is made available under aCC-BY 4.0 International license.

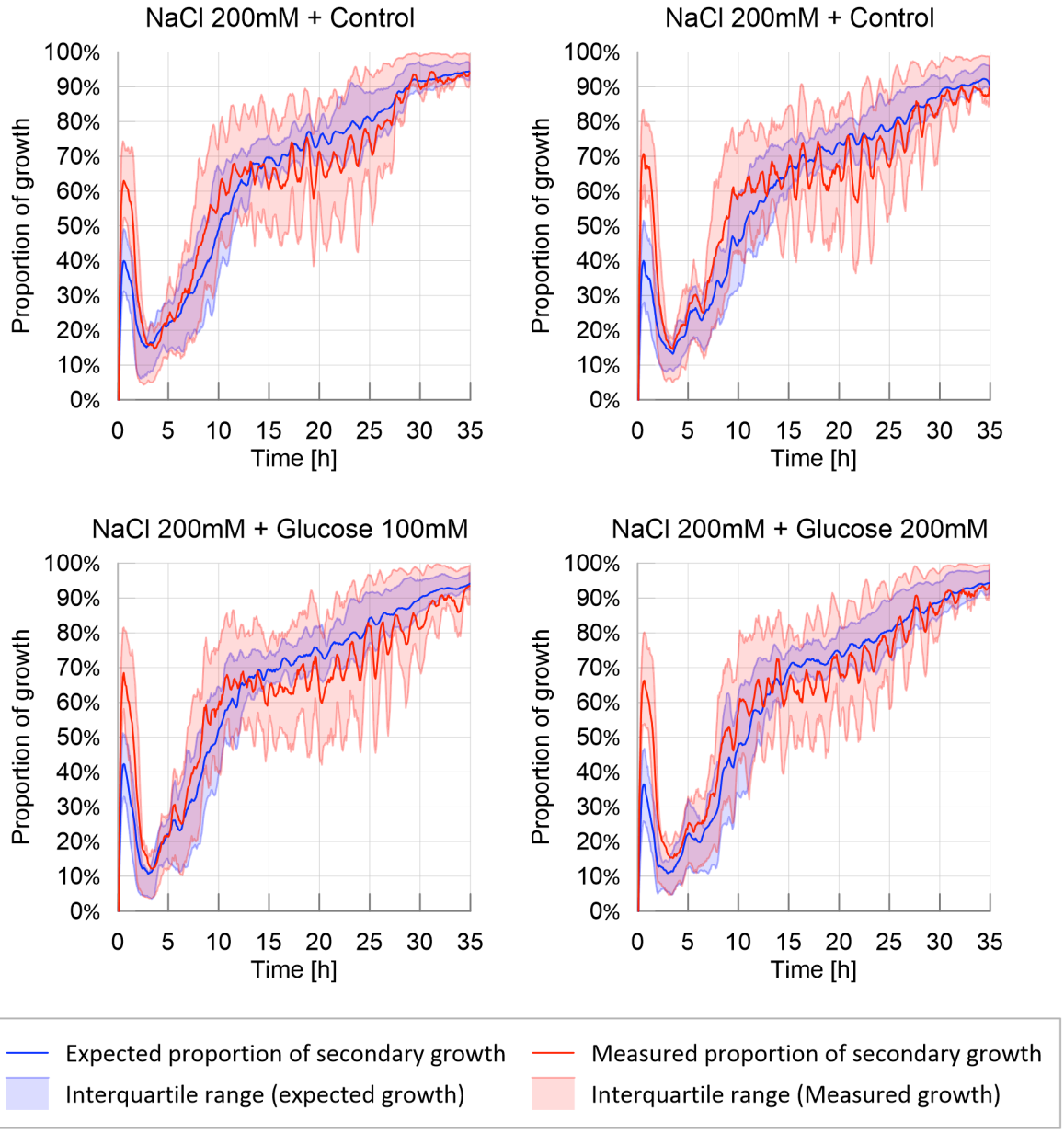

Fig 11: Probability of secondary growth: observed and expected proportion of secondary growth. The solid line corresponds to the average calculated over 20 replicates per treatment, while the shaded areas correspond to the first and third quartiles of the data.

The results obtained for the four different shape indexes (Fig 4 in S1 Appendix) for the spot experiments support the hypothesis that discrete spots of nutrients or repellents did not affect the overall expansion dynamics and exploration cycles. This interpretation is confirmed by the average number of pseudopods, which was found

bioRxiv preprint doi: https://doi.org/10.1101/622662; this version posted April 29, 2019. The copyright holder for this preprint (which was not certified by peer review) is the author/funder, who has granted bioRxiv a license to display the preprint in perpetuity. It is made available under aCC-BY 4.0 International license.

to be correlated to the formation of mucus during the exploration phase: in all the spot experiments, the number of clusters increases from 1 to 2.5 within around 12 hours, to reach a plateau afterwards. In other words, less exploration cycles were observed in non homogenous environments, yielding less pseudopodia.

The evolution of the shortest distance from the slime mold cell to the glucose spot is shown in Fig 12, which can be viewed as a "survival" plot, displaying the proportion of the replicate (P) in which slime mold has not reached the nutritive spot at a given time. Both increasing the concentration of nutrient in the spot (from slightly nutritive to highly nutritive) and adding an aversive spot increased the time to reach the food patch by decreasing the probability to reach it (time to food patch: Table 22 and Fig 18 in S1 Appendix, nutritive: $P < 0.01$; aversive: $P < 0.05$).

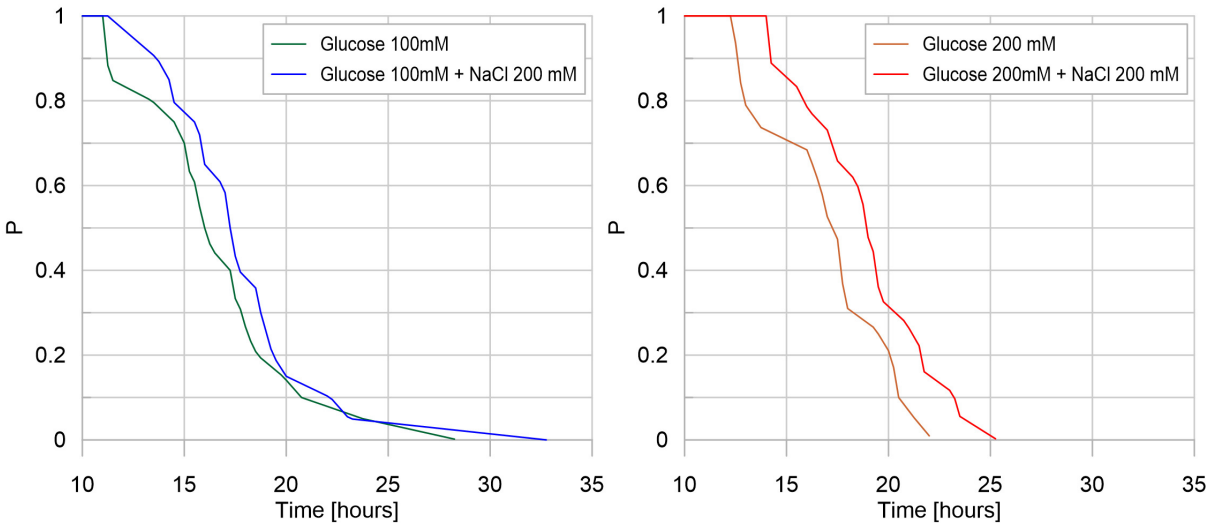

Fig 12. Survival plot: glucose concentration effect. For each treatment, on the vertical axis, the value P corresponds to the fraction of replicates that have not reached the glucose spot at a given time. For a representative number of replicates, P is the probability that glucose has not been reached by slime mold at a given time, for a specific treatment. On the horizontal axis, each value of time corresponds to the average time it takes for a certain fraction of slime mold (P) to reach the glucose spot.

bioRxiv preprint doi: https://doi.org/10.1101/622662; this version posted April 29, 2019. The copyright holder for this preprint (which was not certified by peer review) is the author/funder, who has granted bioRxiv a license to display the preprint in perpetuity. It is made available under aCC-BY 4.0 International license.

Discussion

Exploration in slime molds involves two different processes: area extension and movement (27). Slime molds locomotion and morphogenesis depend on the response of the organism to the environmental conditions. In the present paper, we show that distributions of nutritive and aversive cues affected drastically the exploration pattern of slime molds.

The typical exploration behavior of a slime mold (control condition) started by a stretching period where the slime molds grew uniformly in all directions for 10 hours. Then, the contour of slime mold lost circularity when the first pseudopodia appeared, which also corresponds to the first occurrence of mucus. This phenomenon is typical of the directed digitated growth, or branching phase, described by numerous authors (27,51,59–61). Slime molds developed multiple pseudopodia and did not exhibit any preferential exploration orientation. At the end of the experiment, almost all the arena was explored by the slime mold. Thus the exploration was characterized by three phases: (i) Primary growth only, in the quasi-absence of mucus (5-10 hours); (ii) Combination of primary and secondary growth; (iii) Secondary growth only, when the slime mold stops exploring new substrate areas.

1) Homogeneous distribution of nutritive cues

First, we noted that an environment containing a uniform distribution of nutrients slowed down the exploration of slime mold, mainly by delaying secondary growth and increasing the period of the pulsatile exploration/refinement movements. The

bioRxiv preprint doi: https://doi.org/10.1101/622662; this version posted April 29, 2019. The copyright holder for this preprint (which was not certified by peer review) is the author/funder, who has granted bioRxiv a license to display the preprint in perpetuity. It is made available under aCC-BY 4.0 International license.

414 area not explored by the slime molds was 3 times larger (respectively 7 times larger)
415 than in the environment deprived of nutrient (control case) for a slightly nutritive
416 (respectively highly nutritive) environment. The exploration rate was almost linear for
417 highly nutritive environments, while for other treatments, the area covered by the
418 slime molds reached a plateau after a period of stretching, which indicates
419 secondary growth and slime mold displacement. This means that slime molds that
420 explored nutritive environments never exhibited a Phase (iii) in their exploration
421 pattern.
422 Second, on substrates with higher nutrient concentrations, the slime molds grew in a
423 more compact fashion, *i.e*. slime molds presented the highest solidity index and the
424 lowest number of pseudopodia (clusters). Additionally, the appearance of mucus,
425 which indicates that the slime mold was withdrawing, occurred much later in nutritive
426 environments. As glucose is only aversive when only above 300mM (54), our results
427 suggest that nutritive media depressed migration due to feeding behavior. This
428 allows the organism to remain at a site until nutrients are exhausted (54,62,63). In
429 previous studies, it was shown that the area of substrate covered increases when
430 slime mold responds to nutrient dilution (54,64). Here, we confirmed these
431 observations and noted that slime mold tended to migrate and grow faster on
432 substrates with the lowest concentration of nutrients, thus maximizing nutrient intake
433 and optimizing the trade-off between nutrient foraging and nutrient intake.
434
435 **2) Homogeneous distribution of aversive cues**
436
437 The aversion of slime mold to salt manifested itself through longer contemplative
438 behavior, delayed primary growth and a higher probability to crawl on previously

bioRxiv preprint doi: https://doi.org/10.1101/622662; this version posted April 29, 2019. The copyright holder for this preprint (which was not certified by peer review) is the author/funder, who has granted bioRxiv a license to display the preprint in perpetuity. It is made available under aCC-BY 4.0 International license.

explored surface. In addition, the slime molds grew more compactly and with less pseudopods. This suggests that slime molds were actively avoiding contact with the aversive surface (44,49). In the absence of cell walls, slime mold has no other protection from the environment than mucus. Indeed, in bacteria for instance, mucus is used as protective barrier for the cells against harsh external conditions (65). In slime molds, the extracellular mucus excreted by the slime molds can have different roles: hydrophilic shield to prevent water loss (66), a lubricating surface over which the slime molds can easily crawl (67), a defensive coat to protect against invasion by foreign materials and organisms (66,68), an aid to phagocytosis (69), a surface that promotes ion-exchange (66) and has externalized spatial memory that helps navigation in unknown environments (26,36,53). Here, we can add a new function for the mucus i.e. a buffer to move in adverse environment.

3) Non-Homogeneous distribution of aversive and non aversive cues

In the spot experiments, pulsatile movements were limited and slime molds responded in the same way regardless of the concentration of glucose used as attractant and regardless of the presence of a salt spot on the way to the glucose spot. Slime molds grew in a more compact fashion, *i.e*. slime molds presented the highest solidity index and the lowest number of pseudopodia (clusters). Additionally, the evolution of the areas covered by slime mold and mucus over time indicates that the response of slime molds to heterogeneous environments was similar to that in the control case. This result suggests that in the spot experiments, the exploration behavior of slime mold is mostly controlled by the substrate. Our observation confirms that salt reception can be affected by the presence of sugars (46). The

bioRxiv preprint doi: https://doi.org/10.1101/622662; this version posted April 29, 2019. The copyright holder for this preprint (which was not certified by peer review) is the author/funder, who has granted bioRxiv a license to display the preprint in perpetuity. It is made available under aCC-BY 4.0 International license.

464 authors in (46) showed that the “apparent” enthalpy change accompanying salt
465 perception decreases with increase of sugar concentration.
466
467 The proposed image analysis program allows extracting information on expansion
468 rates, geometric changes and probability of occupancy. Ongoing developments aim
469 to acquire high quality images of slime mold exploration tests and to expand the
470 code’s capabilities to extract topological information on the networks formed by slime
471 molds. Possible applications of the code go beyond the study of slime molds. For
472 instance, the analysis of successive images of an ant nest could allow detecting the
473 generation of any rhythmic activity. Trajectories of individuals within a flock could
474 also be described to understand whether or not members of the flock can inform and
475 influence the travel direction of other individuals. Such a finding would allow
476 understanding how group decisions are made among gregarious species. The
477 cluster identification and shape recognition program could be used to differentiate
478 modes of gene expression or to recognize objects. Object identification is an
479 important pillar to explain associative memory or to track species interactions in an
480 ecosystem. The tools and approach presented here are thus applicable to any
481 problem of network dynamics or pattern recognition.
482

483 Methods

484 1) Species

485 *Physarum Polycephalum,* also known as the true slime mold, belongs to the
486 Amoebozoa, the sister group to fungi and animals (50). Slime molds are found on
487 organic substrates like tree bark or forest soil where they feed on microorganisms
488 such as bacteria or fungi (50). The vegetative morph of *P. polycephalum*, the

bioRxiv preprint doi: https://doi.org/10.1101/622662; this version posted April 29, 2019. The copyright holder for this preprint (which was not certified by peer review) is the author/funder, who has granted bioRxiv a license to display the preprint in perpetuity. It is made available under aCC-BY 4.0 International license.

plasmodium, is a vast multinucleate cell that can grow to cover up to a few square meters and crawl at speeds from 0.1 to few centimeters per hour (29,30). When hygrometry and food availability decrease, the plasmodium turns into an encysted resting stage made of desiccated spherules called sclerotium (29).

2) Rearing conditions

Experiments were initiated with a total of 10 sclerotia per strain (Southern Biological, Victoria, Australia). We cultivated slime molds on a 1% agar medium with rolled oat flakes, slime molds were fed every day and the medium was replaced daily. Slime molds were 2 weeks old when the experiment started. All experiments were carried out in the dark at 25°C temperature and 70% humidity, and ran for 35 h. Pictures were taken every 5 min with a Canon 70D digital camera.

3) Experimental setup

Initially we monitored the exploration movement evoked in slime molds in a homogeneous environment. Each slime mold was placed in the center of a circular arena (14.5cm in diameter) with a layer of agar (1% in water) mixed with non-nutritive cellulose (5%). Adding cellulose to the agar mix proved to be useful to obtain a homogeneous pigmentation and to enhance the color contrast between the substrate and slime mold, therefore improving the identification process. A circular hole (2.5cm in diameter) was punched and replaced with a circular slime mold of the same size sitting on oat. In the first and second treatments (nutritive environments) we added glucose (100mM or 200mM) to the medium. In the third treatment (adverse environment), we added a known repellent (NaCl 100mM (51)) to the medium. Lastly, in the fourth treatment, the medium remained unchanged (neutral environment *i.e.* control treatment).

bioRxiv preprint doi: https://doi.org/10.1101/622662; this version posted April 29, 2019. The copyright holder for this preprint (which was not certified by peer review) is the author/funder, who has granted bioRxiv a license to display the preprint in perpetuity. It is made available under aCC-BY 4.0 International license.

Subsequently, to investigate how chemotaxis modified the exploration behavior, we introduced discrete spots of attractants/repellants within a neutral substrate made of plain agar. In these so-called “spot experiments”, we followed a procedure similar to that for the homogeneous environments. A circular slime mold (2.5 cm in diameter) was placed diametrically opposite to a glucose (attractant) spot of same size placed 4.5cm away. In some of the treatments, a salt (NaCl 200mM, repellent) spot was added at the center of the petri dish. A total of 4 different treatments were tested: the first and the second with a single spot of glucose at concentrations of 100mM and 200mM respectively, the third and fourth keeping the glucose spots with the same concentrations and adding a NaCl 200mM spot at the center of the dish.

All slime molds were fed just before the experiment so we assumed that they were in the same physiological state. The experiment consisted of a total of 8 different treatments. We replicated the experiment 20 times for each treatment and monitored each arena for 35 hours taking time-lapse photographs every 5 minutes. Fig 13 shows the experimental set-up for homogeneous environments (left) and discrete distributions of attractants/repellants (right).

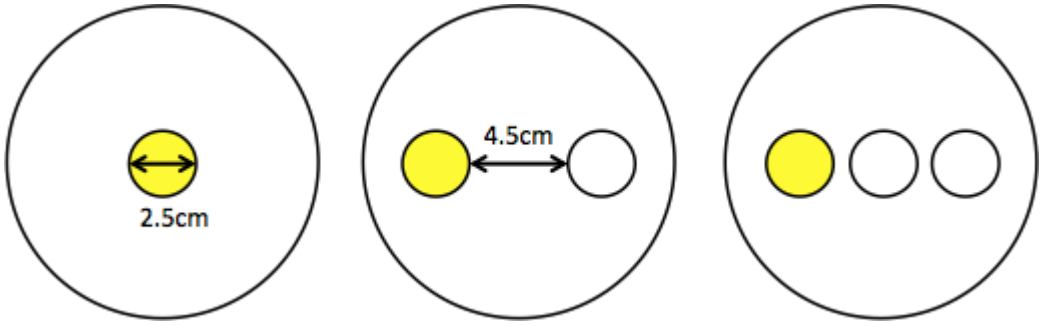

Fig 13: Experimental set-ups for homogenous environment and spot experiment

bioRxiv preprint doi: https://doi.org/10.1101/622662; this version posted April 29, 2019. The copyright holder for this preprint (which was not certified by peer review) is the author/funder, who has granted bioRxiv a license to display the preprint in perpetuity. It is made available under aCC-BY 4.0 International license.

534 **4) Image Processing**

535 Time-lapse images were taken every 5 minutes for a total of 420 pictures for each
536 replicate. The images acquired initially belong to the RGB color space and their size
537 was 1200 by 1200 pixels. Image analysis followed three main steps. First, the edge
538 of the petri dish was identified by fitting its border to a circle of known diameter.
539 Second, the image was segmented using the clustering algorithm k-means (52),
540 which was applied to the images converted into the ab* color space, which is the
541 CLAB space without the L* (lighting) component; this choice corresponds to the
542 robustness of this color space against changes of lighting conditions between
543 images. By the end of this step, all the pixels inside petri dish, e.g. the region of
544 interest (ROI), are identified as either slime mold or not-slime mold.
545
546 After distinguishing slime mold and non-slime mold areas, we identified the mucus
547 by using a subtraction method. The mucus is left by slime after refinement; this
548 substance acts as a marker present on already explored areas of the domain,
549 serving as an external memory to the slime mold (36,53). The fact that this mucus is
550 transparent makes it very challenging to identify by sole color analysis. We thus
551 trinarized the image based on the history of a given pixel, since a pixel that is
552 classified as non-slime-mold at the current image will necessarily contain mucus if it
553 has ever been classified as slime mold in any of the previous images. Conversely, a
554 non-slime-mold pixel will be classified as unexplored substrate if it has never hosted
555 slime mold up to that point in time.
556
557 The change of class from unexplored substrate to slime mold, defined as primary
558 growth, means that a new sprout of the slime mold reaches a point in space that it

bioRxiv preprint doi: https://doi.org/10.1101/622662; this version posted April 29, 2019. The copyright holder for this preprint (which was not certified by peer review) is the author/funder, who has granted bioRxiv a license to display the preprint in perpetuity. It is made available under aCC-BY 4.0 International license.

had never explored before. Similarly, secondary growth is defined as the change from mucus to slime mold, meaning that the slime mold is revisiting an already explored location. Lastly, if the slime mold recedes from a point, e.g. a pixel goes from slime mold to non-slime mold, it becomes mucus, and the process is defined as refinement. By the end of these three steps, the images have been trinarized, meaning that every pixel is classified as slime mold, unexplored substrate, or mucus (and the points outside the ROI are disregarded). Two videos are provided to the reader as supplementary material, S2 and S3 show one of the replicates as original images and trinarized images after identification respectively.

5) Image Analysis in Space and Time

After completing the trinarization, we calculated several indexes to characterize slime mold geometry dynamics. We averaged the indexes over the 20 replicates of each treatment in order to obtain statistically representative measures, and we plotted them over time.

In order to quantify the differences of slime mold spreading dynamics on distinct substrates, we first calculated the fraction of the petri dish area covered by slime mold, mucus and unexplored substrate over time. The total area, the lighting conditions and the test duration were the same for all treatments, both in the homogeneous and spot experiments. Note that glucose only provides energy to slime mold, which is not gaining significant mass during the experiments (54). In other words, slime mold is changing its area by mostly by stretching and contracting, therefore changing its area density.

bioRxiv preprint doi: https://doi.org/10.1101/622662; this version posted April 29, 2019. The copyright holder for this preprint (which was not certified by peer review) is the author/funder, who has granted bioRxiv a license to display the preprint in perpetuity. It is made available under aCC-BY 4.0 International license.

In order to gain further insights about the exploration process we then computed the cumulative area of primary growth, refinement, and secondary growth over the full period of the experiments comparing two consecutive images at the time. The cumulative area covered by primary growth is indicative of the total area of exploration, therefore it is always smaller or equal to the total area of the dish. The cumulative area covered by secondary growth indicates whether slime mold expansion is monotonic (dominated by primary growth) which results in a smaller magnitude, or cyclic (secondary growth dominated, with pulsatile movements) which results in a larger magnitude. The cumulative area covered by refinement indicates slime mold density changes. Within a given time interval, if the area covered by primary plus secondary growth equals that covered by refinement, then slime mold keeps the same density, whereas if it is superior, the slime mold stretches (e.g. density decreases). If secondary growth is negligible and if the area covered by primary growth equals the area covered by refinement, then slime mold displaces mass.

We next measured the migration rate. To this aim, for two consecutive images, we measured the distance from each pixel where growth occurred (both primary and secondary) to the closest pixel classified as slime mold in the previous image. This distance represents the extent of growth from one image to the next. We calculated the migration rate as the ratio between the maximum distance traveled and the time interval between two images (5 min). This maximum distance traveled was then used to delineate the region explored by slime mold within the 5 min interval. In other words, we defined an area of interest as the contour of the slime mold with an offset

bioRxiv preprint doi: https://doi.org/10.1101/622662; this version posted April 29, 2019. The copyright holder for this preprint (which was not certified by peer review) is the author/funder, who has granted bioRxiv a license to display the preprint in perpetuity. It is made available under aCC-BY 4.0 International license.

609 corresponding to the maximum distance traveled (see Fig 1 in S1 Appendix for more
610 details).
611
612 We estimated the fraction of secondary growth as the ratio between the number of
613 pixels changing from mucus to slime mold and the total number of pixels in the
614 region of interest. We then calculated the fraction area of "expected secondary
615 growth", which would have occurred if secondary growth had happened randomly. If
616 the measured secondary growth fraction is higher (respectively, lower) than the
617 expected one, this means that slime mold has a bias towards mucus (respectively,
618 unexplored substrate).
619
620 Additionally, we computed four shape parameters indicative of the contour of slime
621 mold: circularity, eccentricity, solidity and number of clusters. Circularity (C) is
622 defined as:

$$C = {P^2}/{4\pi A}$$

623 Where P and A are the perimeter and area of the shape of slime mold at a given
624 time; this index is equal to one when the contour of slime mold is circular, and
625 increases as the shape deviates from the circle. Eccentricity (E) is calculated as the
626 ratio between the distance between the foci and the major axis length, as follows:

$$E = \sqrt{1 - \left(\frac{b}{a}\right)^2}$$

627 In which *a* and *b* are the lengths of the major and minor axes, respectively. When E
628 is equal to zero, the contour is a circle; when E is equal to one, the contour is
629 degenerated into a line. Solidity (S) is the ratio between the area of the slime mold
630 contour and the area of its convex hull, e.g. the smallest convex polygon that

bioRxiv preprint doi: https://doi.org/10.1101/622662; this version posted April 29, 2019. The copyright holder for this preprint (which was not certified by peer review) is the author/funder, who has granted bioRxiv a license to display the preprint in perpetuity. It is made available under aCC-BY 4.0 International license.

encloses all the slime mold pixels. S is equal to unity when the contour shape is convex. Lastly, we measured the number of clusters by performing an “erosion” operation along the contour of the slime mold, consisting in removing the veins that connect the regions of high concentration of slime mold. After this erosion process, only the clusters of high concentration of slime mold remained, which provided the number of pseudopodia at the given image.

For the spot experiments, we also determined the distance from the slime mold to the glucose spot at every time step. This distance was calculated as the minimum distance between the contour of the slime mold and the perimeter of the glucose circular spot. The evolution of the distance to glucose over time was analyzed in a way similar to a survival analysis, as described below.

5) Statistics

The full description of the statistics is provided as part of the supplementary information; Appendix S1 includes the results of the complete statistical analyses, while appendix S4 gives the necessary instructions to reproduce those analyses. When dependent variables lasted until the occurrence of certain event, we conducted survival analyses using the R package coxme (55). For the remaining dependent variables, we did linear analyses using the R packages lme4 (56) and lmerTest (57). For the experiments done in homogeneous environment, we tested the four different treatments (control, nutritive and adverse) as fixed factors. For the spot experiments, we tested the effect of the nature of the nearest spot (neutral or NaCl 200mM) and that of the furthest spot (glucose 100mM or 200mM), as well as

bioRxiv preprint doi: https://doi.org/10.1101/622662; this version posted April 29, 2019. The copyright holder for this preprint (which was not certified by peer review) is the author/funder, who has granted bioRxiv a license to display the preprint in perpetuity. It is made available under aCC-BY 4.0 International license.

656 the interaction between the two. We always considered the date of the experiment
657 as a random factor as all treatments were conducted over multiple days, with several
658 replicates per day for each treatment. For each statistical analysis, we performed a
659 nested model comparison using the R package MuMIn (58) by ordering models
660 according to their Akaike criterion. We represented the selected model by plotting
661 estimators with the pairwise comparison (a posteriori Tuckey test) p-values using the
662 R package emmeans (58) in linear models, and the hazard ratio associated p-values
663 in cox models.
664

665 ## Supporting information

666

667 **S1 Appendix. Supplementary information: Image analysis and statistical**
668 **results.** Description of the methodology to extract indexes from image analysis and
669 results obtained from the statistical analysis that support our observations**.**

670 **S2 Video. Time-lapse of one experiment replicate, original images.** Video
671 showing the evolution of the slime mold cell over the 35 hours of the experiments,
672 original acquired photos.

673 **S3 Video. Time-lapse of one experiment replicate, trinarized images.** Time
674 lapse of the results of the image segmentation for the same experiment shown in S2
675 Video.

676 **S4 Appendix. Statistic analysis script description.** Step by step description of the
677 procedure followed to generate the results of the shown statistical analyses.

678

679

bioRxiv preprint doi: https://doi.org/10.1101/622662; this version posted April 29, 2019. The copyright holder for this preprint (which was not certified by peer review) is the author/funder, who has granted bioRxiv a license to display the preprint in perpetuity. It is made available under aCC-BY 4.0 International license.

680 ## Acknowledgements

681

682 This work was supported by the U.S National Science Foundation, under grant
683 CMMI#1552368: “CAREER: Multiphysics Damage and Healing of Rocks for
684 Performance Enhancement of Geo-Storage Systems - A Bottom-Up Research and
685 Education Approach.” A.D. and A.B. were supported by a grant from the Agence
686 Nationale de la Recherche (reference number: ANR-17-CE02-0019-01 -SMART-
687 CELL).

688

689

690

691

692

693

694

695

696

697

698

699

700

701

702

703

704

bioRxiv preprint doi: https://doi.org/10.1101/622662; this version posted April 29, 2019. The copyright holder for this preprint (which was not certified by peer review) is the author/funder, who has granted bioRxiv a license to display the preprint in perpetuity. It is made available under aCC-BY 4.0 International license.

705 # References

706

707 1. Ball P, Borley NR. The self-made tapestry: pattern formation in nature. Vol.
708 198. Oxford University Press Oxford; 1999.
709 2. Rietkerk M, de Koppel J. Regular pattern formation in real ecosystems. Trends
710 Ecol Evol. 2008;23(3):169–75.
711 3. Theraulaz G, Gautrais J, Camazine S, Deneubourg J-L. The formation of
712 spatial patterns in social insects: from simple behaviours to complex
713 structures. Philos Trans R Soc London Ser A Math Phys Eng Sci.
714 2003;361(1807):1263–82.
715 4. Teague BP, Guye P, Weiss R. Synthetic morphogenesis. Cold Spring Harb
716 Perspect Biol. 2016;8(9):a023929.
717 5. Goodwin BC. Unicellular morphogenesis. Cell Shape Determ Regul Regul
718 Role. 1989;365–91.
719 6. Chalut KJ, Paluch EK. The actin cortex: a bridge between cell shape and
720 function. Dev Cell. 2016;38(6):571–3.
721 7. Driscoll MK, McCann C, Kopace R, Homan T, Fourkas JT, Parent C, et al. Cell
722 shape dynamics: from waves to migration. PLoS Comput Biol.
723 2012;8(3):e1002392.
724 8. Salbreux G, Charras G, Paluch E. Actin cortex mechanics and cellular
725 morphogenesis. Trends Cell Biol. 2012;22(10):536–45.
726 9. Charras G, Sahai E. Physical influences of the extracellular environment on
727 cell migration. Nat Rev Mol cell Biol. 2014;15(12):813.
728 10. van Helvert S, Storm C, Friedl P. Mechanoreciprocity in cell migration. Nat Cell
729 Biol. 2018;20(1):8.

bioRxiv preprint doi: https://doi.org/10.1101/622662; this version posted April 29, 2019. The copyright holder for this preprint (which was not certified by peer review) is the author/funder, who has granted bioRxiv a license to display the preprint in perpetuity. It is made available under aCC-BY 4.0 International license.

730 11. Friedl P, Wolf K. Plasticity of cell migration: a multiscale tuning model. J Cell
731 Biol. 2010;188(1):11–9.
732 12. Gardel ML, Schneider IC, Aratyn-Schaus Y, Waterman CM. Mechanical
733 integration of actin and adhesion dynamics in cell migration. Annu Rev Cell
734 Dev Biol. 2010;26:315–33.
735 13. Inagaki N, Katsuno H. Actin waves: Origin of cell polarization and migration?
736 Trends Cell Biol. 2017;27(7):515–26.
737 14. Aman A, Piotrowski T. Cell migration during morphogenesis. Dev Biol.
738 2010;341(1):20–33.
739 15. Reig G, Pulgar E, Concha ML. Cell migration: from tissue culture to embryos.
740 Development. 2014;141(10):1999–2013.
741 16. Yamada KM, Mayor R. Cell dynamics in development, tissue remodelling, and
742 cancer. Curr Opin Cell Biol. 2016;42:iv.
743 17. Hind LE, Vincent WJB, Huttenlocher A. Leading from the back: the role of the
744 uropod in neutrophil polarization and migration. Dev Cell. 2016;38(2):161–9.
745 18. Mseka T, Bamburg JR, Cramer LP. ADF/cofilin family proteins control
746 formation of oriented actin-filament bundles in the cell body to trigger fibroblast
747 polarization. J Cell Sci. 2007;120(24):4332–44.
748 19. King JS, Insall RH. Chemotaxis: finding the way forward with Dictyostelium.
749 Trends Cell Biol. 2009;19(10):523–30.
750 20. Iglesias PA, Devreotes PN. Navigating through models of chemotaxis. Curr
751 Opin Cell Biol. 2008;20(1):35–40.
752 21. Larsen SH, Adler J, Gargus JJ, Hogg RW. Chemomechanical coupling without
753 ATP: the source of energy for motility and chemotaxis in bacteria. Proc Natl
754 Acad Sci. 1974;71(4):1239–43.

bioRxiv preprint doi: https://doi.org/10.1101/622662; this version posted April 29, 2019. The copyright holder for this preprint (which was not certified by peer review) is the author/funder, who has granted bioRxiv a license to display the preprint in perpetuity. It is made available under aCC-BY 4.0 International license.

22. Nakaoka Y, Iwatsuki K. Hyperpolarization-activated inward current associated with the frequency increase in ciliary beating of Paramecium. J Comp Physiol A. 1992;170(6):723–7.

23. Saranak J, Foster KW. Rhodopsin guides fungal phototaxis. Nature. 1997;387(6632):465.

24. Nakagaki T, Yamada H, Tóth A. Maze-solving by an amoeboid organism. Nature [Internet]. 2000;407(6803):470. Available from: http://www.ncbi.nlm.nih.gov/pubmed/11028990

25. Kuroda S, Takagi S, Nakagaki T, Ueda T. Allometry in Physarum plasmodium during free locomotion: size versus shape, speed and rhythm. J Exp Biol. 2015;218(23):3729–38.

26. Rodiek B, Hauser MJB. Migratory behaviour of Physarum polycephalum microplasmodia. Eur Phys J Spec Top. 2015;224(7):1199–214.

27. Vogel D, Nicolis SC, Perez-Escudero A, Nanjundiah V, Sumpter DJT, Dussutour A. Phenotypic variability in unicellular organisms: from calcium signalling to social behaviour. Proc R Soc B Biol Sci. 2015;282(1819):20152322.

28. Vogel D, Dussutour A, Deneubourg J-L. Symmetry breaking and inter-clonal behavioural variability in a slime mould. Biol Lett. 2018;14(12):20180504.

29. Aldrich H. Cell biology of Physarum and Didymium V1: organisms, nucleus, and cell cycle. Elsevier; 2012.

30. Oettmeier C, Brix K, Döbereiner H-G. Physarum polycephalum—A new take on a classic model system. J Phys D Appl Phys. 2017;50(41):413001.

31. Ueda T. Pattern dynamics in cellular perception. Phase Transitions A Multinatl J. 1993;45(2–3):93–104.

bioRxiv preprint doi: https://doi.org/10.1101/622662; this version posted April 29, 2019. The copyright holder for this preprint (which was not certified by peer review) is the author/funder, who has granted bioRxiv a license to display the preprint in perpetuity. It is made available under aCC-BY 4.0 International license.

780 32. Kuroda R, Kuroda H. Relation of cytoplasmic calcium to contractility in
781 Physarum polycephalum. J Cell Sci. 1982;53(1):37–48.
782 33. Yoshimoto Y, Matsumura F, Kamiya N. Simultaneous oscillations of Ca2+
783 efflux and tension generation in the permealized plasmodial strand of
784 Physarum. Cell Motil. 1981;1(4):433–43.
785 34. Farr DR, Amster H, Horisberger M. Composition and partial structure of the
786 extracellular polysaccharide of Physarum polycephalum. Carbohydr Res.
787 1972;24(1):207–9.
788 35. Sesaki H, Ogihara S. Secretion of slime, the extracellular matrix of the
789 plasmodium, as visualized with a fluorescent probe and its correlation with
790 locomotion on the substratum. Cell Struct Funct. 1997;22(2):279–89.
791 36. Reid CR, Latty T, Dussutour A, Beekman M. Slime mold uses an externalized
792 spatial “memory” to navigate in complex environments. Proc Natl Acad Sci.
793 2012;109(43):17490–4.
794 37. Reid CR, Beekman M. Solving the Towers of Hanoi - how an amoeboid
795 organism efficiently constructs transport networks. J Exp Biol [Internet].
796 2013;216:1546–51. Available from:
797 http://www.ncbi.nlm.nih.gov/pubmed/23307798
798 38. Ueda T, Hirose T, Kobatake Y. Membrane biophysicsdf chemoreception and
799 taxis in the plasmodium of physarum polycephalum. Biophys Chem.
800 1980;11(3–4):461–73.
801 39. Reid CR, Latty T. Collective behaviour and swarm intelligence in slime moulds.
802 FEMS Microbiol Rev. 2016;40(6):798–806.
803 40. Saigusa T, Tero A, Nakagaki T, Kuramoto Y. Amoebae anticipate periodic
804 events. Phys Rev Lett. 2008;100(1):18101.

bioRxiv preprint doi: https://doi.org/10.1101/622662; this version posted April 29, 2019. The copyright holder for this preprint (which was not certified by peer review) is the author/funder, who has granted bioRxiv a license to display the preprint in perpetuity. It is made available under aCC-BY 4.0 International license.

41. Tero A, Takagi S, Saigusa T, Ito K, Bebber DP, Fricker MD, et al. Rules for biologically inspired adaptive network design. Science [Internet]. 2010 Jan 22 [cited 2018 Nov 21];327(5964):439–42. Available from: http://www.ncbi.nlm.nih.gov/pubmed/20093467

42. Latty T, Beekman M, Biernaskie J, Walker S, Gegear R, Boivin G, et al. Slime moulds use heuristics based on within-patch experience to decide when to leave. J Exp Biol [Internet]. 2015;218(Pt 8):1175–9. Available from: http://www.ncbi.nlm.nih.gov/pubmed/25722006

43. Reid CR, Garnier S, Beekman M, Latty T. Information integration and multiattribute decision making in non-neuronal organisms. Anim Behav. 2015;100:44–50.

44. Boisseau RP, Vogel D, Dussutour A. Habituation in non-neural organisms: evidence from slime moulds. Proc R Soc B Biol Sci. 2016;283(1829):20160446.

45. Dussutour A, Ma Q, Sumpter D. Phenotypic variability predicts decision accuracy in unicellular organisms. Proc R Soc B. 2019;286(1896):20182825.

46. Terayama K, Ueda T, Kurihara K, Kobatake Y. Effect of sugars on salt reception in true slime moldPhysarum polycephalum. J Membr Biol. 1977;34(1):369–81.

47. Carlile MJ. Nutrition and chemotaxis in the myxomycete Physarum polycephalum: the effect of carbohydrates on the plasmodium. Microbiology. 1970;63(2):221–6.

48. Ueda T, Terayama K, Kurihara K, Kobatake Y. Threshold phenomena in chemoreception and taxis in slime mold Physarum polycephalum. J Gen Physiol. 1975;65(2):223–34.

bioRxiv preprint doi: https://doi.org/10.1101/622662; this version posted April 29, 2019. The copyright holder for this preprint (which was not certified by peer review) is the author/funder, who has granted bioRxiv a license to display the preprint in perpetuity. It is made available under aCC-BY 4.0 International license.

830 49. Ueda K, Takagi S, Nishiura Y, Nakagaki T. Mathematical model for
831 contemplative amoeboid locomotion. Phys Rev E. 2011;83(2):21916.
832 50. Stephenson SL, Schnittler M. Myxomycetes. Handb Protists. 2017;1405–31.
833 51. Vogel D, Dussutour A. Direct transfer of learned behaviour via cell fusion in
834 non-neural organisms. Proc R Soc B Biol Sci. 2016;283(1845):20162382.
835 52. Kanungo T, Mount DM, Netanyahu NS, Piatko CD, Silverman R, Wu AY. An
836 efficient k-means clustering algorithm: Analysis and implementation. IEEE
837 Trans Pattern Anal Mach Intell. 2002;(7):881–92.
838 53. Reid CR, Beekman M, Latty T, Dussutour A. Amoeboid organism uses
839 extracellular secretions to make smart foraging decisions. Behav Ecol.
840 2013;24(4):812–8.
841 54. Dussutour A, Latty T, Beekman M, Simpson SJ. Amoeboid organism solves
842 complex nutritional challenges. Proc Natl Acad Sci. 2010;107(10):4607–11.
843 55. Therneau T. A Package for Survival Analysis in S. version 2.38. 2015.
844 56. Bates D, Sarkar D, Bates MD, Matrix L. The lme4 package. R Packag version.
845 2007;2(1):74.
846 57. Kuznetsova A, Brockhoff PB, Christensen RHB. lmerTest package: tests in
847 linear mixed effects models. J Stat Softw. 2017;82(13).
848 58. Barton K, Barton MK. Package 'MuMIn'Version 1. 2015;
849 59. Halvorsrud R, Wagner G. Growth patterns of the slime mold Physarum on a
850 nonuniform substrate. Phys Rev E. 1998;57(1):941.
851 60. Nakagaki T, Yamada H, Ueda T. Interaction between cell shape and
852 contraction pattern in the Physarum plasmodium. Biophys Chem.
853 2000;84(3):195–204.
854 61. Latty T, Beekman M. Food quality affects search strategy in the acellular slime

bioRxiv preprint doi: https://doi.org/10.1101/622662; this version posted April 29, 2019. The copyright holder for this preprint (which was not certified by peer review) is the author/funder, who has granted bioRxiv a license to display the preprint in perpetuity. It is made available under aCC-BY 4.0 International license.

855 mould, Physarum polycephalum. Behav Ecol. 2009;20(6):1160–7.
856 62. Knowles DJC, Carlile MJ. The chemotactic response of plasmodia of the
857 myxomycete Physarum polycephalum to sugars and related compounds.
858 Microbiology. 1978;108(1):17–25.
859 63. Daniel JW, Baldwin HH. Methods of culture for plasmodial myxomycetes. In:
860 Methods in Cell Biology. Elsevier; 1964. p. 9–41.
861 64. Takamatsu A, Takaba E, Takizawa G. Environment-dependent morphology in
862 plasmodium of true slime mold Physarum polycephalum and a network growth
863 model. J Theor Biol. 2009;256(1):29–44.
864 65. Nwodo U, Green E, Okoh A. Bacterial exopolysaccharides: functionality and
865 prospects. Int J Mol Sci. 2012;13(11):14002–15.
866 66. McCormick JJ, Blomquist JC, Rusch HP. Isolation and characterization of a
867 galactosamine wall from spores and spherules of Physarum polycephalum. J
868 Bacteriol. 1970;104(3):1119–25.
869 67. Simon HL, Henney HR. Chemical composition of slime from three species of
870 myxomycetes. FEBS Lett. 1970;7(1):80–2.
871 68. Asgari M, Henney JHR. Inhibition of growth and cell wall morphogenesis of
872 Bacillus subtilis by extracellular slime produced by Physarum flavicomum.
873 Cytobios. 1977;20(79–80):163–77.
874 69. Haskins EF, Hinchee AA. Light-and ultra-microscopical observations on the
875 surface structure of the protoplasmodium, aphanoplasmodium, and
876 phaneroplasmodium (Myxomycètes). Can J Bot. 1974;52(8):1835–9.
877